COMPARISON OF RAIN/NO-RAIN CLASSIFICATION METHODS OVER LAND FOR TRMM MICROWAVE IMAGER

Shinta Seto*, Nobuhiro Takahashi, and Toshio Iguchi

National Institute of Information and Communications Technology, Tokyo, Japan

1. INTRODUCTION

To improve the rainfall retrieval accuracy of the microwave imagers is particularly important over land where the retrieval accuracy is currently unsatisfactory, especially given the widespread demand from various communities for the application of rainfall observation data to flood alert and water management systems. Over land, the emission algorithm (e.g., Wileheit, 1977) is useless because emission from rain drops is largely hidden by the warm land surface. Hence, a scattering algorithm, using a higher frequency (around 85 GHz), is used for rainfall retrieval over land (e.g., Spencer *et al*. 1983). When a scattering algorithm is applied over land, variations in the observed brightness temperature caused by land surface conditions must be distinguished from variations caused by precipitation. Land surfaces covered by desert sand or fallen snow produce lower brightness temperatures because sand and snow particles on the ground scatter microwave radiation at a higher frequency. If this phenomenon is not distinguished from scattering by solid precipitation, it leads to false estimates of rainfall over desert and snow-covered areas.

In general precipitation retrieval algorithms, the rain/no-rain classification (RNC) is applied after quality checks and land/ocean classification and before the actual retrieval. RNC assigns a deterministic flag for “rain” or “no-rain” to observations; then, only observations with a “rain” flag are processed in the retrieval algorithm. We propose new rain/no-rain classification (RNC) methods that take into account multi-scale spatial and temporal variations in land surface brightness temperatures. We therefore summarize TMI data observed under no-rain conditions to produce a statistical database of land surface brightness temperatures. In this paper, we propose new RNC methods based on this database.

2. DATA

The standard products of PR and TMI (version 5) are used in this study. The period of analysis is from 1998 to 2000, before the change in orbital altitude. Data given by PR products, including surface-type flags from 2A21, rain flag, rain type and storm height from 2A23, and the near-surface rain rate from 2A25 (Iguchi *et al*., 2000), were used in this study. Data given by TMI, including brightness temperature from 1B11, and surface and rain flags from 2A12 (Kummerow *et al*., 2001), were also used.

Corresponding author address: 4-2-1, Nukui-Kita-Machi, Koganei-Shi, Tokyo, JAPAN, 184-8795; e-mail: seto@nict.go.jp

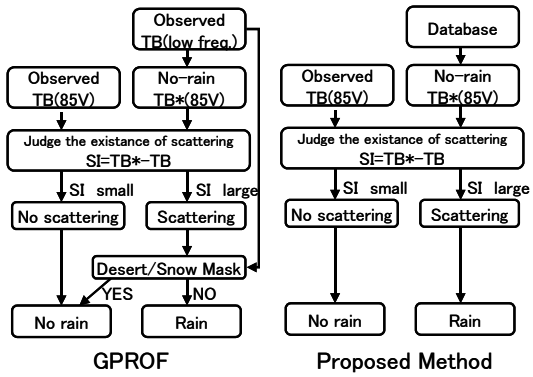

Fig. 1. Schematic of RNC methods in GPROF and methods proposed in this study

3. RAIN/NO-RAIN CLASSIFICATION METHOD

3.1. RNC Method of GPROF

RNC method over land for GPROF Version5 (Goddard profiling algorithm), which is the standard algorithm for TMI, is explained. First, the existence of scattering was assessed. The observed brightness temperature of 85 V (denoted as TB (85 V)) is compared with the estimated TB (85 V) without the scattering effects of precipitation (hereafter, TB*(85 V)); the difference is calculated as SI=TB*(85 V)-TB (85 V), where SI is an abbreviation of Scattering Index. In the case of GPROF, TB*(85 V) is simply set at the observed TB (22 V). When SI is larger than 8 [K], the observation is classified as “scattering”. Otherwise, it is classified as “no scattering” (Fig. 1).

In the second step, desert and snow-covered regions are removed from the “scattering” data by the use of lower frequency observations. To detect desert regions, polarization differences in the brightness temperature at 19 GHz, TB (19 P)=TB

(19 V)-TB (19 H) are utilized (P indicates "polarization"). The principle of the detection is that TB (19 P) for desert is large because there is less volume scattering by vegetation. In contrast, 22 V is used to detect fallen snow. On the principle that physical temperatures and brightness temperatures are low when the land surface is covered by snow, data with a low TB (22 V) is judged as "scattering by fallen snow" which means "no rain".

3.2. RNC Methods Proposed by This Study

Our proposed RNC methods also calculate SI=TB*(85 V)-TB (85 V). While GPROF estimates B*(85 V) using observed brightness temperature at lower frequency we use a statistical database to determine TB*(85 V).

We focused on quasi-simultaneous observations by PR and TMI to select brightness temperature data under no precipitation conditions. As shown in Fig. 2, PR observations, the center of which are in a TMI footprint in the case of 85 GHz, are used as references for TMI observations. When all the PR observations within a TMI footprint have a "no rain" or "rain possible" flag, the TMI observation is judged to be under a no-rain condition. TMI brightness temperature data observed under no-rain conditions are summarized in the database with resolutions of one month and $1^\circ \times 1^\circ$ (latitude-longitude). The average and standard deviation of TB (85 V) are calculated to represent the distribution and they are stored in the database. In addition, the coefficients of the linear regression lines between TB (85 V) and TB (22 V) are stored in the database.

We propose two RNC methods (M1 and M2) for real-time use and two RNC methods (M1+ and M2+) for post-processing. M1 and M1+ refer to the average μ and standard deviation σ from the corresponding grid of the database. TB*(85 V) is set at μ and the threshold for SI is set at $k_0 \times \sigma$, where k_0 is a constant in time and space. M2 refers to the linear regression line between TB (85 V) and TB (22 V) as shown in equation (1) from the corresponding grid of the database.

$$\text{TB (85 V)}_{\text{no-rain}} = a + b \times \text{TB (22 V)}_{\text{no-rain}} \quad (1)$$

The observed TB (22 V) is substituted into equation (1) and TB*(85 V) is found as shown in equation (2).

$$\text{TB (85 V)}^* = a + b \times \text{TB (22 V)}_{\text{obs}} \quad (2)$$

The threshold of SI is set at $k_0 \times \sigma_e$, where σ_e is the standard deviation of the residuals of the regression. In an evaluation of one month in 2000, a database for the same month in 1998 and 1999 was used in M1 and M2, while a database for the same month in 2000 was used in M1+ and M2+. M1+ and M2+ cannot be applied in real-time use and is tried here to provide a comparison with M1 and M2, respectively. Our proposed methods do not require screening for desert and snow cover, and thus require only one step for "rain" or "no-rain" classification using SI (Fig. 1)

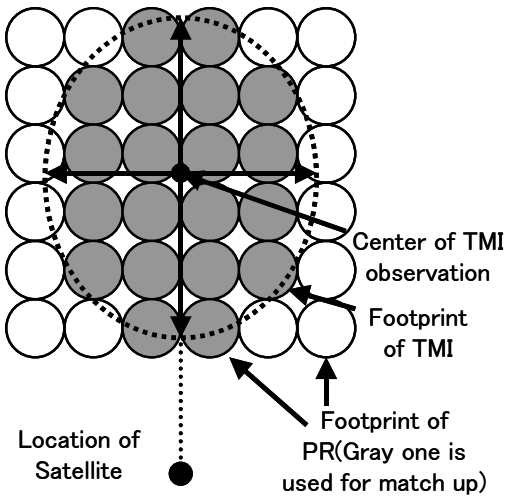

Fig. 2. Match-up between PR and TMI. Gray PR pixels provide references for TMI observations.

4. EVALUATION OF RNC

In the same way, to separate no-rain TMI observations to produce the database described in section 3.2, the RNC for the TMI footprint (85 GHz) is determined by PR. Combinations of RNC results are categorized by A to D (A---"rain" by PR and "rain" by TMI. B---"rain" by PR and "no-rain" by TMI. C---"no-rain" by PR and "rain" by TMI". D--- "no-rain" by PR and "no-rain" by TMI). In the evaluation, the following three indices were calculated.

RTDO＝(Number of occurrences in A)/{(Number of occurrences in A)+(Number of occurrences in B)}
RTDA＝(Total amount of rain rate in A)/{(Total amount of rain rate in A)+ (Total amount of rain rate in B)}
RFAO＝(Number of occurrences in C)/{(Number of occurrences in C)+(Number of occurrences in D)}

where RTDO, RTDA, and RFAO are abbreviations for the ratio of true detection (occurrence base), ratio of true detection (amount base), and ratio of false alarms (occurrence base), respectively. The "rain rate" used to calculate RTDA is the averaged "near-surface rain rate" given in the standard product 2A25 of PR to the TMI footprint (85 GHz). Each RNC is evaluated only when the surface flags for both PR and TMI are "land".

5. COMPARISON OF METHODS

5.1. General Comparison

Evaluation indices for all the TMI observations in 2000 are compared for M1, M2, M1+, M2+, and GPROF in Fig. 3. The ideal results are maximum RTDO (RTDA)=1 and minimum RFAO=0. Generally, these two purposes are not accomplished at once, because the distribution of TB under "no-rain" condition and that under "rain" condition are overlapped. When RTDO increases, RFAO decreases and vice versa. The RTDO, RTDA, and RFAO for GPROF are 59%, 80%, and 0.85%, respectively. To realize as small a RFAO as GPROF, k_0 must be set to 2.8 and 3.5 for M1 and M2, respectively. The RTDO is 57% and 63% for M1 and M2, and the RTDA is 81% and 86% for M1 and M2, respectively, in this case. GPROF is superior to M1 in terms of the RTDO, but M1 is superior to GPROF in terms of the RTDA. There is little difference in the RTDO (RTDA) for M1 and M1+ (M2 and M2+) for the same k_0; however, M1+ (M2+) produced a smaller RFAO than M1 (M2).

5.2. Comparison between M1 and M1+: Effects of Interannual Variation

The RFAO for M1 is much larger than that of M1+ because of interannual variation in the distribution of "no-rain" brightness temperatures for present and past data. When the threshold of the TB for M1 is higher than that for M1+, the RFAO and RTDO for M1 are larger. Conversely, a lower threshold for M1 results in a small RFAO and RTDO for M1 compared with M1+. Both cases can happen as a result of interannual variation, but the increase in the RFAO with a larger threshold is much greater than the decrease in the RFAO with a smaller threshold because the "no-rain" probability density function is an increasing function of the TB around the threshold. Unless the interannual variation has significant bias, the RFAO for the total evaluation is larger for M1 than for M1+. In contrast, the "rain" probability density function can be an increasing or decreasing function around the threshold. Therefore, both the increase in the RTDO with a higher threshold, and its decrease with a lower threshold are almost cancelled. Consequently, the difference in the RTDO between M1 and M1+ is not large. As above, M1 is inferior to M1+ due to the interannual variations of land surface brightness temperatures.

5.3. Comparison between M1 and M2: Effects of Diurnal Variations

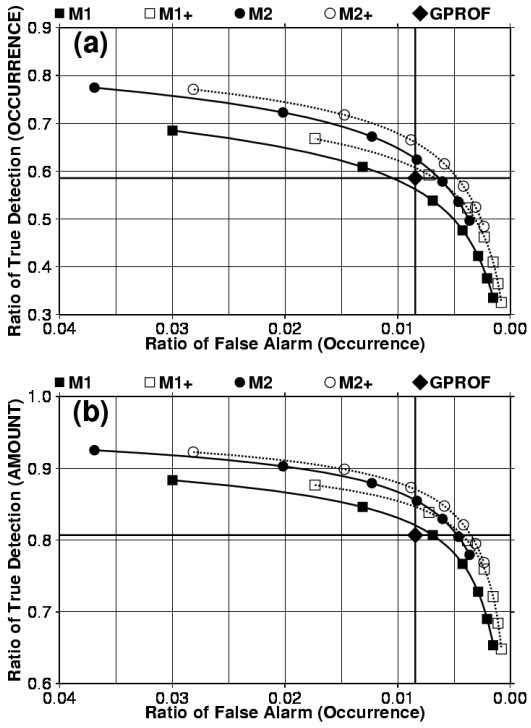

Fig. 3. Evaluations of RNC methods (M1, M1+, M2, M2+, and GPROF) for the total test. The abscissa is RFAO. The ordinate is (a) RTDO and (b) RTDA.

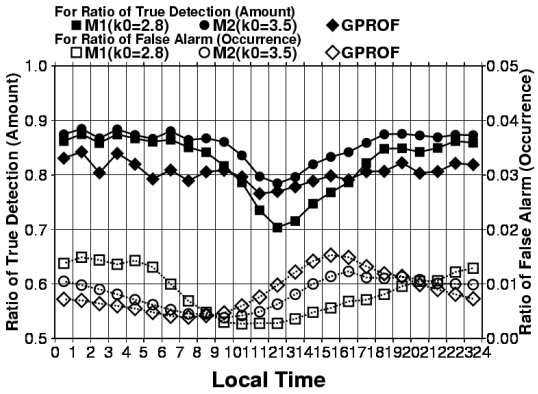

Fig. 4. Relationship between local time and RTDA/RFAO for M1, M2, and GPROF.

The difference of accuracies between M1 and M2 is due to diurnal variations in the RTDA and RFAO (Fig. 4). For M1, both the RFAO are much higher at night than in the daytime. In other words, at night, M1 judges a larger number of observations as "rain" than M2 and GPROF. "No-rain" brightness temperatures are lower at night due to diurnal variations in the physical temperature of the land surface; thus, the constant threshold for the TB produces a higher RFAO at night. These artificial diurnal variations in RTDA and RFAO disappeared in M2 by

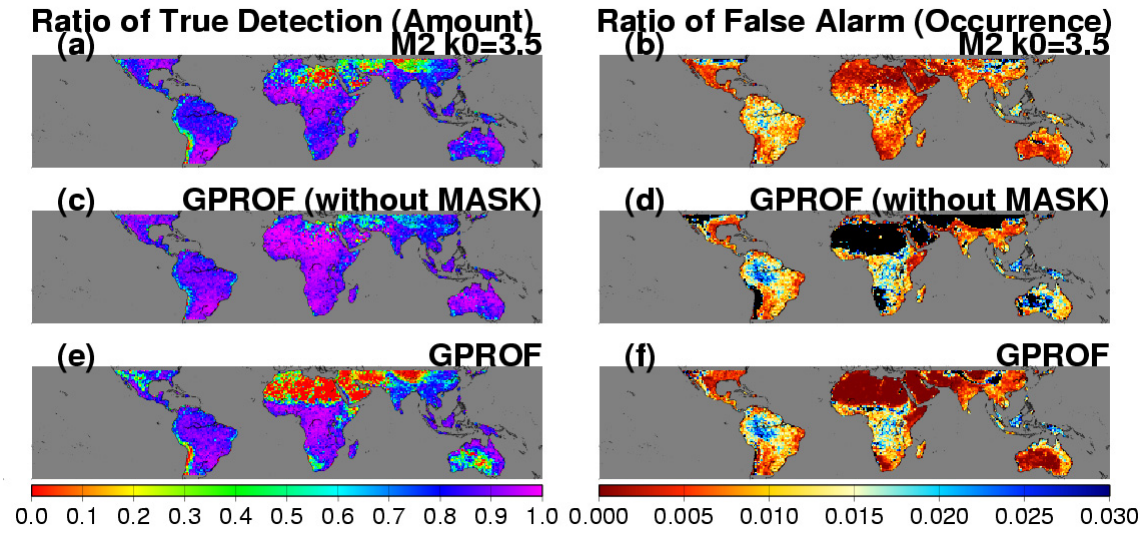

Fig. 5. Spatial distribution of (a), (c), and (e) RTDA, and (b), (d), and (f) RFAO. (a) and (b) for M2, (c) and (d) for GPROF without desert and snow mask, and (e) and (f) for GPROF.

changing TB* (85 V) within a month. The difference between M1 and M2 can be explained as above.

5.4. Comparison between M2 and GPROF: Detection of Precipitation over Desert and Snow-Covered Areas

The distribution maps of the RTDA and RFAO for GPROF (without desert/snow screening), GPROF (with desert/snow screening) and M2 are shown in Fig. 5. Without the screening process, the RFAO for GPROF is quite high for desert and snow-covered regions, while the RTDA is satisfactory for all areas. In contrast, the RFAO for M2 is low, even for desert and snow-covered regions. This is because the database referred to by M2 has information on when and where scattering occurs as a result of desert and snow cover. To decrease the RFAO in desert and snow-covered areas, GPROF has to use a screening process. After screening is applied, the RFAO is almost zero for desert and snow-covered areas, but the screening process also decreases the RTDA severely in these areas. For example, the RTDA for GPROF is low for the Sahara desert, inland areas of the Australian Continent, the Middle East, and the Tibetan Plateau compared with that of M2. The difference between GPROF and M2 in the accuracy of the RNC mainly comes from these regions.

6. SUMMARY

To produce a consistent database under no rain conditions, space-borne precipitation radar is essential. Without TRMM-like satellites, such a database cannot be produced globally. Data from a two-year period were used to produce the database in this study, but this period is not long enough to remove sampling bias. If we used data from a longer period for the construction of database, the accuracy of the database could be further improved. An expanded database would also partly compensate for differences between M1 and M1+ (M2 and M2+). For GPM observations, a database could be produced using TRMM observations over six years.

Acknowledgements. This study is part of a larger study, “Production of a high-precision, high-resolution global precipitation map using satellite data (GSMaP)” led by Prof. Ken’ichi Okamoto (Osaka Prefecture University, Japan) under the program, “Core Research for Evolutional Science and Technology (CREST)” of the Japan Science and Technology Agency (JST).

REFERENCES

Iguchi, T., *et al*., 2000: Rain-profiling algorithm for the TRMM precipitation radar. *J. Appl. Meteor.*, **39**, 2038-2052.

Kummerow, C., *et al*., 2001: The evolution of the Goddard profiling algorithm (GPROF) for rainfall estimation from passive microwave sensors. *J. Appl. Meteor.*, **40**, 1801-1820.

Spencer, R. W., *et al*., 1983: Satellite microwave radiances correlated with radar rain over land. *Nature*, **304**, 141-143.

Wilheit, T. T., *et al*., 1977: A satellite technique for quantitatively mapping rainfall rates over the oceans. *J. Appl. Meteor.*, **16**, 551-560.